Macromolecules

Article

Cite This: Macromolecules 2017, 50, 8480-8486

pubs.acs.org/Macromolecules

A Highly Soluble, Fully Aromatic Fluorinated 3D Nanostructured Ladder Polymer

Lilian I. Olvera,[†] Manuel Rodríguez-Molina,[†] F. Alberto Ruiz-Treviño,[§] Mikhail G. Zolotukhin,*[,†] Serguei Fomine,[†] Jorge Cárdenas,[‡] Rubén Gaviño,[‡] Larissa Alexandrova,[†] Rubén A. Toscano,[‡] and Eduardo Martínez-Mercado[§]

[†]Instituto de Investigaciones en Materiales and [‡]Instituto de Química, Universidad Nacional Autónoma de México, Apartado Postal 70-360, CU Coyoacán, 04510 México D. F., México

[§]Departamento de Ingeniería y Ciencias Químicas, Universidad Iberoamericana, Prol. Paseo de la Re-forma No. 880, 01219 México D.F., México

ABSTRACT: A new, high-molecular-weight, aromatic fluorinated ladder polymer has been obtained by the superacid-catalyzed, nonstoichiometric, step polymerization of a xanthenediol with trifluoroacetone. The polymerizations carried out at room temperature in a mixture of trifluoromethanesulfonic acid (CF_3SO_3H, TFSA) with methylene chloride resulted in a polymer completely soluble in acetone, methylene chloride, chloroform, THF, methanol, DMF, NMP, and DMAC. The chemical composition of the ladder polymer has been confirmed by the complementary experimental and calculations studies of the ^{13}C and ^{19}F NMR spectra and the calculations of reaction pathways. It was also found that the growth of the fully fused-ring backbone polymer chain occurs in all three dimensions due to the formation of regioisomeric fragments. Appropriate films, for the determination of gas permeation coefficients, were obtained by casting. According to gas permeation experiments, the ladder polymer falls above Robeson's 2008 updated upper bound for the O_2/N_2 gas pair.

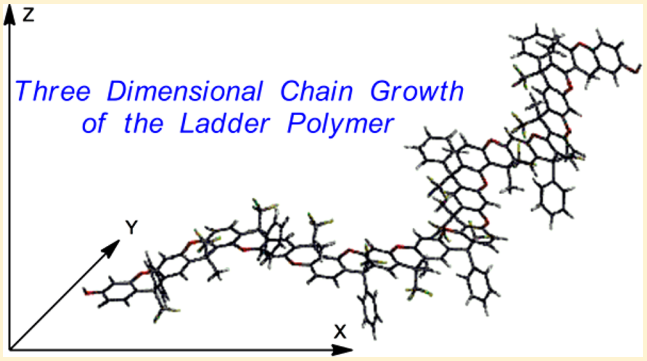

INTRODUCTION

Ladder polymers,[1,2] defined as an "uninterrupted series of rings connected by sterically restrictive links around which rotation cannot occur without the breaking of a bond", comprise a special topic in polymer science.

In the initial phase of the history of ladder polymers they were mostly considered as ideal candidates for applications requiring materials with high thermal, mechanical, and chemical stability.

Since the mid-1980s, there has been ever increasing interest in the electrophysical and optical properties of ladder polymers possessing a planarized π-electron system which ensures optimum electron delocalization.

The high rigidity of ladder polymers, in combination with a loose chain packing, has proved to be an important factor for generating an unusually high microporosity that leads to polymer membranes with significant improvements in both gas permeability coefficients and selectivity for several gas pairs, as it has been learned from the evaluation of the gas transport properties in spiro, ladder, or MOP (microporous organic polymer) polymers reported elsewhere.[3−9]

In regards to syntheses of ladder polymers, more and more publications have appeared. It is beyond the scope of this paper to cover all the history and chemistry of ladder polymers, which are well documented in reviews and original papers (see some of them and references cited therein[10−22]).

However, there are challenging problems in ladder-polymer syntheses. Two special drawbacks are (i) the generally poor solubility of the ladder structures, which inhibits molecular-weight growth, and (ii) the possibility of cross-linking or branching during the polymer-building process. Side reactions of these types cause incomplete ladder formation and drastically decrease the solubility of the products obtained.

The key to defect-free ladders is transformations with complete regioselectivity. Highly specific and efficient reactions with quantitative (or nearly quantitative) yields are absolutely essential to obtain the desired ladder macromolecules.

Recently, efficient TFSA-catalyzed condensations of trifluoromethyl ketones with catechol, resorcinol, and hydroquinone (in the ratio 1 mol of ketone/2 mol of phenol) have been described.[23] Thus, 2,2,2-trifluoroacetophenone reacts with resorcinol in the presence of TFSA at room temperature to give 3,6-dihydroxy-9-trifluoromethyl-9-phenylxanthene in high yield (reaction conditions were not optimized) (Scheme 1).

Received: July 3, 2017
Revised: October 5, 2017
Published: October 30, 2017

DOI: 10.1021/acs.macromol.7b01413
Macromolecules 2017, 50, 8480−8486

Scheme 1. Synthesis of 3,6-Dihydroxy-9-trifluoromethyl-9-phenylxanthene[23]

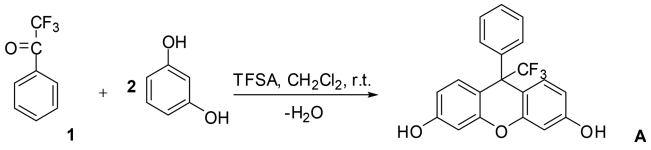

More recently, polymers and copolymers containing 9*H*-xanthene moieties in the backbone were synthesized at room temperature by superacid-catalyzed step-growth polymerizations of carbonyl compounds with bisphenols (Scheme 2).

Scheme 2. Synthesis of Polymers by the Polymerization of Ketones with Bisphenols[24]

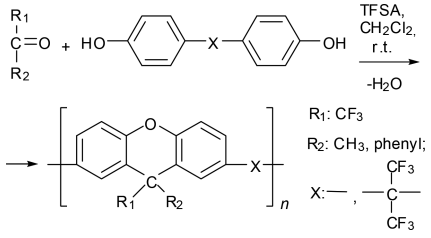

Therefore, it seemed plausible that xanthenediol **A** would react with 2,2,2-trifluoroacetone (in the ratio 1 mol of ketone/1 mol of bisphenol) to form a ladder polymer (Scheme 3).

According to the calculations of reaction pathways,[25] the cyclodehydration in the xanthene syntheses occurs during the hydroxyalkylation step in which the phenyl ring is activated toward nucleophilic aromatic substitution to form an ether bond. In other words, both strands of the ladder structure might be generated in a single reaction.

RESULTS AND DISCUSSION

Polymer Synthesis. 3,6-Dihydroxy-9-trifluoromethyl-9-phenylxanthene (**A**) has been obtained according to the published method.[23] A high-quality crystalline sample of xanthenediol (**A**) was used for data collection and structure refinement. X-ray crystallographic analyses reveals that xanthenediol **A** adopts an overall butterfly like conformation with the central 4*H*-pyran ring in a boat conformation (Figure 1).

Step-polymerization of xanthenediol (**A**) with trifluoroacetone was carried out under conditions similar to the polymerizations of linear bisphenols with trifluoromethyl ketones.[24] Since our initial attempts on the stoichiometric polymerization of the monomers resulted in longer reaction times and oligomeric products, we have performed a nonstoichiometric polymerization of bisphenol with trifluoroacetone. Contrary to the classical theory of step-growth polymerization, the highest molecular weight in superacid-catalyzed polyhydroxyalkylation is achieved when an excess of the carbonyl compound is used.[26] Nonstoichiometric polymerization of trifluoroacetone with xanthenediol **A** (in the ratio 1.3 mol of ketone/1 mol of xanthenediol) in a medium of methylene chloride gave polymeric product in 2 h (Table 1).

Figure 1. Molecular structure of 3,6-dihydroxy-9-trifluoromethyl-9-phenylxanthene.

The reaction solution was poured into water; the yellowish fiber-like powder formed was filtered off, washed copiously with water, and after drying in air reprecipitated twice from acetone into water. Remarkably, the polymer obtained is completely soluble in methylene chloride, chloroform, THF, DMF, NMP, DMAC, THF, and pyridine, and flexible transparent films could be cast from the solutions. Even more surprising is that the polymer is soluble in acetone and methanol, which is very unusual for aromatic polymers. It is very likely that the presence of swivel trifluoromethyl groups, lack of dense polymer packing due to rigid, nonplanar xanthene fragments, and presumably regular polymer structure are the reasons for such high solubility.

Polymer Structure. It is worth mentioning that polymers containing hydroxy groups are generally insoluble in chlorinated solvents. Therefore, solubility of the polymer in chlorinated solvents (and absence of color changes in the presence of the polymer with sodium and potassium hydroxide) points to complete conversion of phenol groups in the cyclodehydration reaction to yield ether bonds. It is noteworthy that in the IR spectrum of the polymer there are no characteristic bands corresponding to hydroxyl groups (3400–3650 cm^{-1}). The bands appeared at 1607 and 1469 cm^{-1} can be assigned to the aromatic C–C double bonds. A characteristic intensive multipeak at 1136 cm^{-1} is attributed to C–O–C stretching vibrations.

Scheme 3. Hypothetical Synthesis of Ladder Polymer

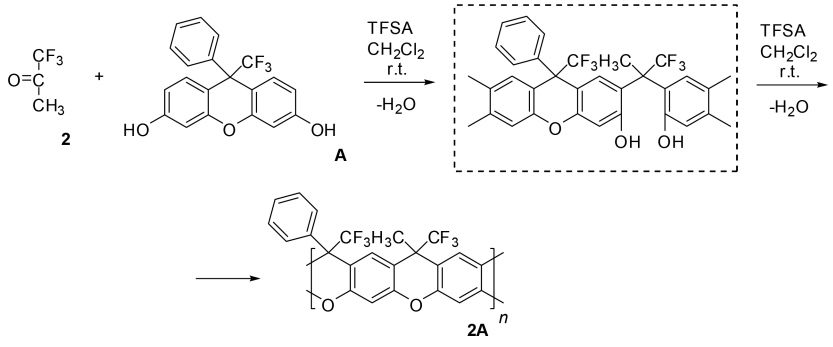

DOI: 10.1021/acs.macromol.7b01413
Macromolecules 2017, 50, 8480–8486

Table 1. Step Polymerization of Trifluoroacetone with Xanthenediol A

entry	reaction conditions[a]	reaction time (h)	η_{inh} (dL/g^{-1})[b]	M_w/M_n (kDa)[c]	PDI (M_w/M_n)	T_g (°C)	T_d (°C)[d]	yield (%)
1	ST	12	0.08	7.22/4.27	1.69	nd	nd	54
2	ST	24	0.14	10.51/4.11	2.57	nd	nd	72
3	NST	2	0.62	41.52/20.99	1.98	>400	473	93

[a]ST: stoichiometric polycondensation. NST: nonstoichiometric polycondensation. [b]0.2% solution in NMP. [c]Molecular weights (M_w, M_n) determined by GPC-MALLS, THF. [d]Onset (°C).

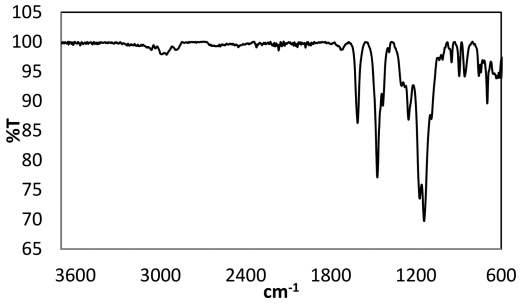

Figure 2. IR spectra of ladder polymer.

In contrast to the clear pattern of the IR spectrum, the ^{1}H NMR spectrum of the polymer is unsuitable for analysis because of overlapping of many signals. It was reported that the folding of xanthene units along the connecting line through the oxygen atom and the xanthene carbon atom C-9 gives rise to the formation of stereoisomers.[24] Obviously, the nonplanar, double-stranded, fully fused-ring backbone ladder structure would produce complicated NMR spectra. Thus, although the ^{13}C NMR spectrum of the polymer allows for the assignment of some main signals of polymer structure, it cannot be accepted as evidence of the ladder structure suggested (Figure 3). It is worth noting that very often the detail structural characterization of ladder polymers is generally considered to be a more difficult task than the synthesis itself. Therefore, we decided to use ^{19}F NMR spectroscopy.

The polymer has only two types of fluorine atoms, which suggests that there should be only two signals in the ^{19}F NMR spectra; however, the reality is quite different. The ^{19}F NMR spectra of the polymer revealed the existence of multiple signals (Figure 4, bottom) spread over 14 ppm.

A similar situation holds for ^{13}C NMR spectra where the number of signals exceeds the number of unique carbon-atom types. This could be a consequence of the lack of stereo- or regioselectivity or both for the polymer forming reaction. To verify this hypothesis, the theoretical calculation of the reaction pathways have been performed.

Calculation of the Reaction Pathways. To explain the origin of multiple signals in NMR spectra of the polymer, nuclear magnetic shielding tensors and chemical shifts of different structures have been calculated using gauge-including atomic orbital method (GIAO)[27] as implemented in Gaussian 09 rev D.01. Dispersion corrected wB97XD functional in combination with triple-ζ quality Ahlrichs basis set was used for these calculations.[28] The lowest energy conformations of oligomers containing six repeat units were used. The chemical shifts (δ) were calculated from the shielding tensors

$$\delta = \sigma_{ref} - \sigma$$

where σ_{ref} is the shielding of $CFCl_3$ predicted by the same methods.

First, different stereoisomers of the oligomer have been calculated (Scheme 4). The results showed that although the stereoisomerism causes splitting of fluorine signals in ^{19}F NMR spectra, the difference between chemical shifts of ^{19}F atoms belonging to different stereoisomer does not exceed a several tenths of ppm. Thus, for all tested stereoisomers the calculated chemical shifts of CF_3-C-Ph and CF_3-C-CH_3 groups were around −79 and −86 ppm, respectively. Therefore, stereoisomerism cannot be the only reason for the multiple fluorine signals.

The reaction between trifluoroacetone and xanthenediol (**A**) can result in the formation of two different structures (see Scheme 4). If the polymer-forming reaction is not regioselective, the polymer chain will contain fragments of different constitutional isomers, which would create a variety of magnetically nonequivalent CF_3 groups. Figure 5 shows the lowest energy conformers of four different hexamers containing different amount of structures I and II, from pure I to pure II.

The second step was the calculation of the magnetic shielding tensors and chemical shifts for these structures. Figure 4 depicts the combined ^{19}F NMR spectra of all four

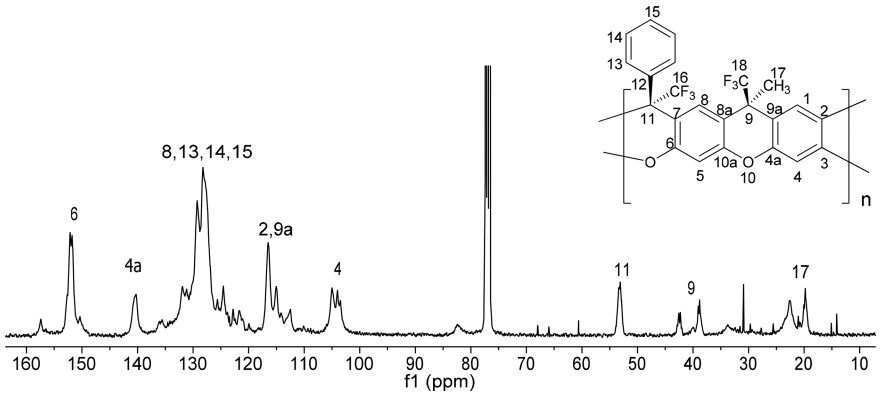

Figure 3. ^{13}C NMR spectrum of ladder polymer **2A** (in $CDCl_3$).

DOI: 10.1021/acs.macromol.7b01413
Macromolecules 2017, 50, 8480−8486

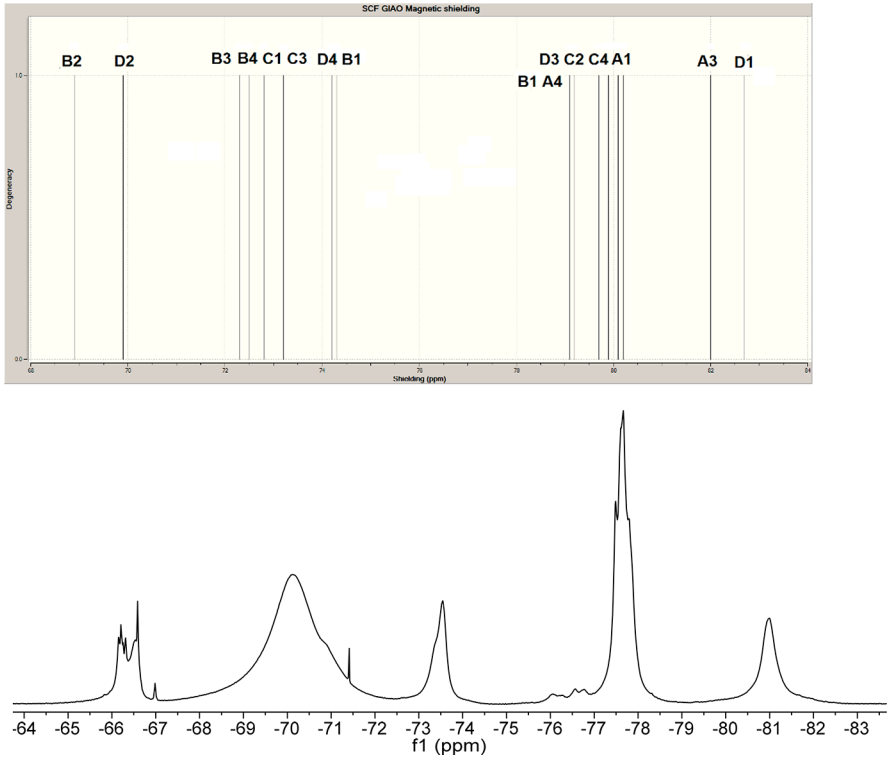

Figure 4. Simulated (top) and experimental (bottom) ^{19}F NMR spectra of the polymer **2A**.

Scheme 4. Possible Formation of Different Constitutional Isomers

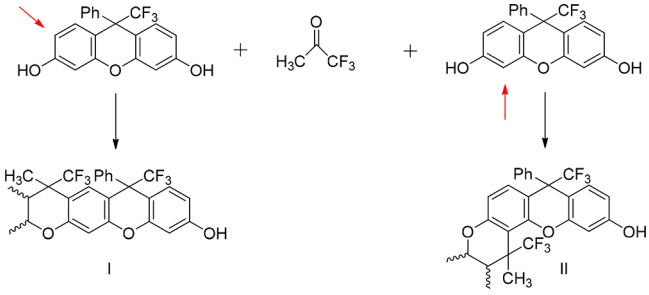

structures and the experimental ^{19}F spectra of the polymer in the range from −70 to −85 ppm. Only four inner repeat units were taken into account to avoid signals originating from terminal groups. A perfect match between the calculated and experimental spectra is not expected, since even in the case of well-defined structures the error is still a few ppm.[29] However, one can predict two important similarities between theoretically calculated and experimental spectra: the first is the spread of the signals, being of about 14 ppm for both the theoretical and experimental spectra; the second is the position of the lowest and the highest field signals, with a difference of only of about 2 ppm. Moreover, the signals of the theoretically calculated spectra are grouped into five multiplets similar to experimental spectra.

As seen, the multiple signals in NMR spectra of the polymer can be explained by assuming the lack of regioselectivity of the polymer-forming reaction. The polymer chain contains both types of fragments: structure I and structure II producing multiple magnetically nonequivalent trifluoromethyl groups. This fact opens up the possibility of manipulating the regioselectivity of the reaction to obtain polymer possessing

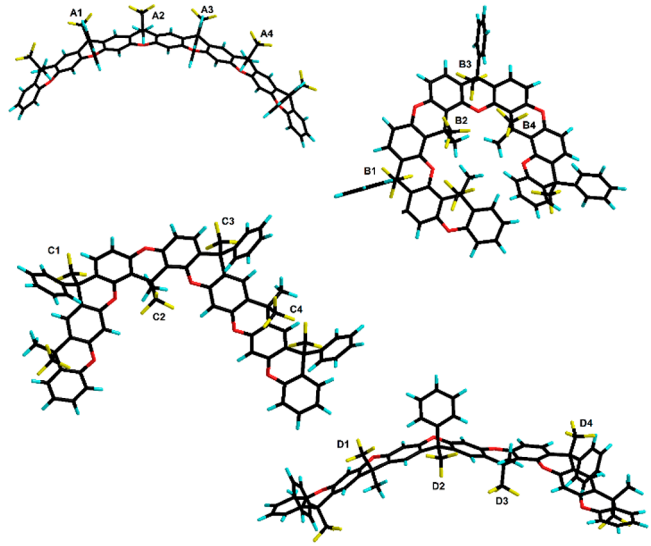

Figure 5. Optimized structures of the lowest energy conformers of studied oligomers.

exclusively either structure I or structure II by modifying only the reaction conditions.

To estimate the selectivity of different reaction sites of xanthenediol, we calculated the free Gibbs activation energies of σ complexes formation for each reaction path (Scheme 5) since this reaction is kinetically controlled. The σ complexes formation was found to be the rate-limiting step for the reaction of TFA with aromatics. We used the same level of theory as in ref 25 which was found to be successful in predicting and explaining the reactivity of other monomers participating in the polyhydroxyalkylation reaction.

DOI: 10.1021/acs.macromol.7b01413
Macromolecules 2017, 50, 8480−8486

Scheme 5. Possible Reaction Pathways in the Reaction of Xanthenediol with Trifluoroacetone

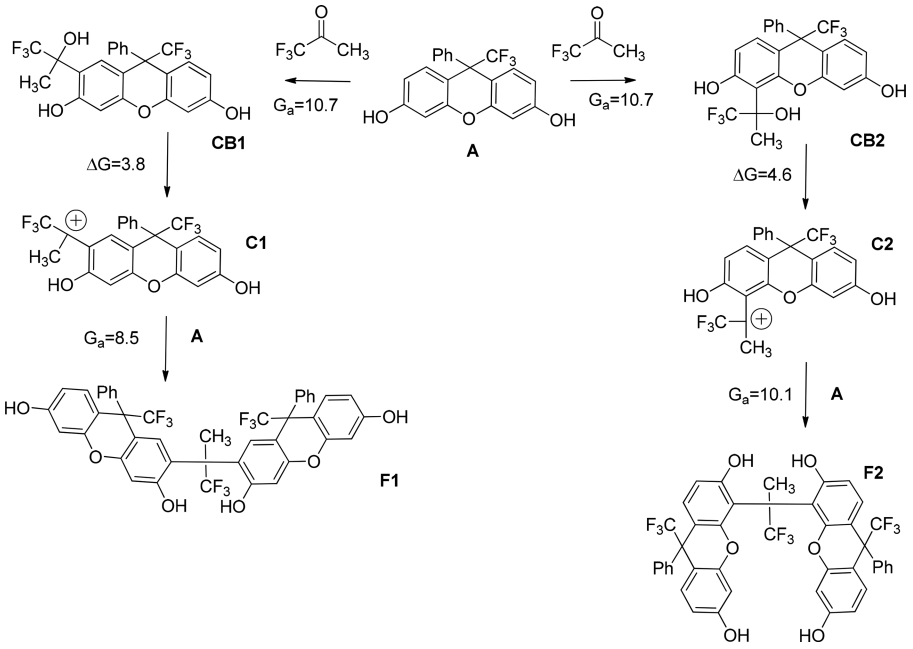

As seen from Scheme 5, the rate-determining step for both reaction paths is the carbinol formation. There is no difference between the activation energies, which suggests that two isomeric carbinols CB1 and CB2 form at the same rate. The next step, the dissociation of carbinols to form carbocations C1 and C2, is a slightly endothermic process with free Gibbs reaction energies of only a few kcal/mol and with no detectable transition states. The last reaction step is the formation of diarylated products F1 and F2, which have close free Gibbs activation energies of 8.5 and 10.1 kcal/mol, respectively. As seen, the formation of carbinols controls the ratio of isomers formed by the electrophilic attacks at positions 2 and 4 of **A**. Considering that there is no difference between two activation energies for the rate-determining step, we expect that the ratio between two isomers should be close to 1:1, which is in agreement with the experimentally observed ^{19}F NMR spectrum (Figure 4).

Therefore, the chemical composition of the polymer obtained can be represented by the structure shown in Scheme 6. It is important to mention that the growth of the fully fused-

Scheme 6. Chemical Composition of Ladder Polymer 2A ($m \approx p$)

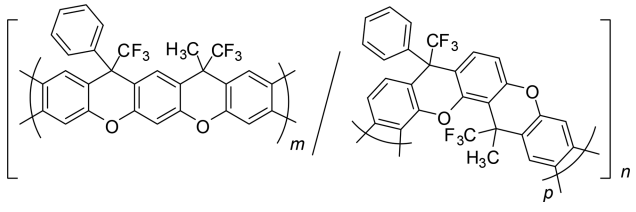

ring backbone polymer chain occurs in all three dimensions due to the formation of regioisomeric fragments. Therefore, the random incorporation of different regioisomers into the polymer chain creates a rigid 3D laddered structure (Figure 6). If it is true, this polymer structure is of particular interest for gas-permeation experiments as it is noted in the following paragraph.

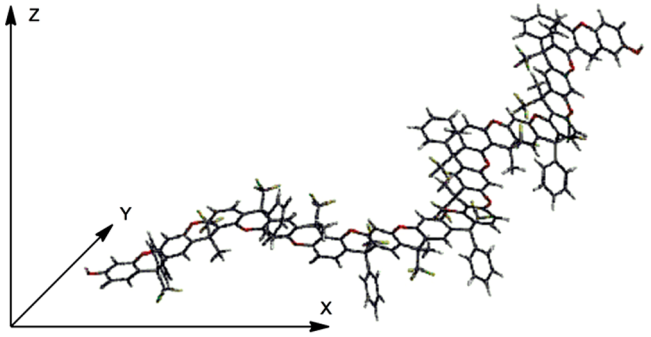

Figure 6. Minimum-energy conformation of ladder polymer segment.

Gas Permeation Experiments. The **2A** ladder polymer is soluble in common solvents and can be easily processed as a solvent-free film to measure its application in different industrial sectors, i.e., as a gas separation medium. Thus, a solvent-free film for gas permeation measurements was formed by solution-casting using a 5 wt % polymer solution in chloroform and then vacuum-drying it at 80 °C for 24 h to eliminate the residual solvent. Films thus obtained proved robust with tensile strength 52.2 ± 7.5 MPa, a Young's modulus of 1350 ± 52 MPa, and elongation at break 12 ± 1.8%. The polymer film, with a 45 μm thickness, was then mounted in a constant-volume/variable pressure permeation cell following a well-established procedure reported elsewhere[30] to measure, at 35 °C and 2 bar upstream pressure, the ultrahigh pure gas permeability coefficient, $P(i)$, for O_2 and N_2. With a $P(O_2)$ in the order of 36.5 barrer, and ideal selectivity for the O_2/N_2 gas pair of 8.5, as reported in Figure 7, its selectivity−permeability combination position it as a promising material for the separation of O_2 and N_2 from air, in a similar manner as the separation performance reported for some other ladder polymers with intrinsic microporosity,[9] i.e., the TPIM-1 and TPIM-2 with aging times higher than 700 days (see Figure 7). Since annealing time is an important variable to describe fractional free-volume variations, i.e., gas separation perform-

DOI: 10.1021/acs.macromol.7b01413
Macromolecules 2017, 50, 8480−8486

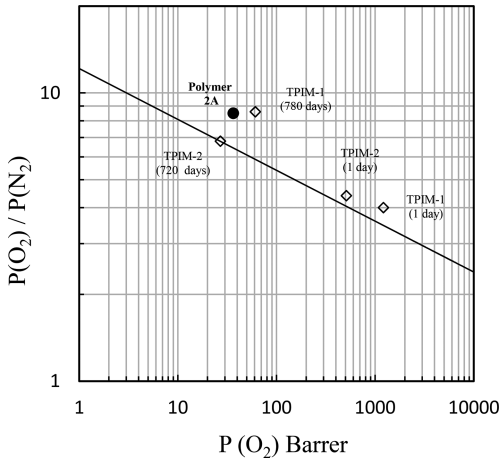

Figure 7. Selectivity–permeability relationship for the gas pair O_2/N_2, measured at 35 °C and 2 bar, in a **2A** polymer membrane (solid circle). Separation performance for other ladder polymers with intrinsic microporosity[9] (open diamonds), T-PIMs "fresh" and "annealed", have been included for comparison purposes. Solid line describes Robeson's 2008 updated upper bound.[31]

ance, it is worthwhile to mention that the separation properties reported for **2A** ladder polymer membranes were measured two months after the film was vacuum-dried. In addition, **2A** polymer was not immersed in methanol as is in the case for the "fresh" and "annealed" PIMs used in Figure 7 for comparison purposes. The attractive ideal selectivity for O_2/N_2 measured for the **2A** ladder polymer should be the result of packing in the solid state a highly nonplanar and rigid structure, as noted in Figures 5 and 6, which arises from an increased intrachain rigidity imposed inside the main polymer repeating unit. The attractive $P(O_2)$ may be the result of either a favorable interaction between the O_2 gas molecule with the oxygen atom in the ether linkage and a relatively high internal free volume shown by this ladder polymer that possess a 587 m^2/g BET surface area as determined from nitrogen adsorption isotherms. Future work will be addressed to the evaluation of the gas separation performance and gas sorption capacity shown by this ladder polymer.

CONCLUSIONS

A metal-free, highly soluble, fully aromatic fluorinated ladder polymer was successfully obtained by one-pot, room-temperature, superacid-catalyzed nonstoichiometric step polymerization of multifunctional monomers xanthenediol and trifluoroacetone. The both strands of the ladder structure are generated in a single reaction. The ladder polymer is completely soluble in common organic solvents, including acetone and methanol, and forms appropriate films, for the determination of gas permeation coefficients, when cast from the solutions. The structure of the polymer was characterized by NMR and FTIR spectroscopies as well as TGA analysis. Complementary experimental and calculations studies of spectral parameters and calculations of reaction pathways revealed the presence of stereo- and regioisomers in the polymer due to nonplanar xanthene fragments and the electrophilic aromatic substitution reactions of ketones in both ortho positions to the hydroxy phenol group. As a result, the growth of the fully fused-ring backbone polymer chain occurs in all three dimensions. Nonplanar, fully fused-ring xanthene backbones and the presence of isomers are favorable for disrupting chain packing and for the development of an apparent high internal free volume as indirectly suggested for the high BET surface area of 587 m^2/g. The significant advantages of this synthetic method are promising synthetic potential, operational simplicity, availability of reactants, and easy work-up.

Gas-permeation experiments have shown that the ladder polymer is a promising material for the membrane gas separation of O_2 and N_2 from air, since the permeability–selectivity combination reported at 35 °C and 2 bar, $P(O_2)$ = 36.5 barrer, and ideal selectivity for O_2/N_2 = 8.5 position it with excellent properties above Robeson's 2008 updated "upper bound".[31] The results obtained also suggest that a large variety of new ladder polymers may be obtained from the polymerization of monomers containing structures with two phenolic hydroxy groups and carbonyl compounds capable of forming xanthenes structures in acid-catalyzed reactions.

EXPERIMENTAL SECTION

Characterization. NMR spectra were taken on Bruker Avance digital spectrometer, operating at 300 and 75 MHz for ^1H and ^{13}C, respectively. Chloroform-d ($CDCl_3$) was used as solvent. Infrared (IR) spectra were measured on a Thermo Scientific Nicolet FT-IR-ATR spectrometer. The inherent viscosities of 0.2% polymer solutions in 1-methyl-2-pyrrolidone (NMP) were measured at 25 °C using an Ubbelohde viscometer. Molecular weights were determined by gel permeation chromatography (GPC–MALLS) according to the published method.[32] Thermogravimetric analyses (TGA) were carried out in air and under nitrogen at a heating rate of 10 °C/min on a DuPont 951 thermogravimetric analyzer.

Materials. All starting materials were obtained from Aldrich. Methylene chloride, 2,2,2-trifluoroacetophenone, and trifluoroacetone were distilled. Trifluoromethanesulfonic acid was distilled prior to use. Resorcinol was used as received.

Synthesis. A mixture of 1,1,1-trifluoroacetone (0.2930 g, 2.6 mmol), 9*H*-xanthene-3,6-diol (0.7166 g, 2.0 mmol), methylene chloride (2.0 mL), and TFMSA (2.0 mL, 22.6 mmol) was stirred at room temperature for 3 h and then poured slowly into water. The precipitated, off-white solid was filtered off, washed several times with water, and dried in air overnight. After the second reprecipitation from acetone into water and drying the resulting white fibrous polymer (**2A**) had an inherent viscosity (η_{inh}) of 0.62 dL/g (in NMP).

AUTHOR INFORMATION

Corresponding Author

*E-mail: zolotukhin@iim.unam.mx (M.G.Z.).

ORCID

Mikhail G. Zolotukhin: 0000-0001-7395-7354

Notes

The authors declare no competing financial interest.

ACKNOWLEDGMENTS

The authors acknowledge the financial support from CONACYT Mexico (Grants 151842, CB-2012-01-184156, and 251693) and from DGAPA-UNAM (PAPIIT IN 105314-3 and IN 203517). Thanks are due to E. R-Morales and S. Morales for assistance with thermal and spectroscopic analysis. The authors also thank A. Lopez Vivas and Alejandro Pompa for technical help. The editorial assistance of Dr. E. S. Wilks is much appreciated.

DOI: 10.1021/acs.macromol.7b01413
Macromolecules 2017, 50, 8480–8486

REFERENCES

(1) IUPAC. Compendium of polymer terminology and nomenclature (Recommendations 2008) (The "Purple Book"). Cambridge, UK, 2009, Chapter 1, Defs. 1.40, 1.41, 1.44 and 1.45.

(2) Winslow, F.; et al. Formation and properties of polymer carbon. *J. Polym. Sci.* **1955**, *16*, 101−120.

(3) Budd, P. M.; Ghanem, B. S.; Makhseed, S.; McKeown, N. B.; Msayib, K. J.; Tattershall, C. E. Polymers of intrinsic microporosity (PIMs): robust, solution-processable, organic nanoporous materials. *Chem. Commun.* **2004**, 230−231.

(4) Budd, P. M.; McKeown, N. B.; Ghanem, B. S.; Msayib, K. J.; Fritsch, D.; Starannikova, L.; Belov, N.; Sanfirova, O.; Yampolskii, Y.; Shantarovich, V. Gas permeation parameters and other physicochemical properties of a polymer of intrinsic microporosity: Polybenzodioxane PIM-1. *J. Membr. Sci.* **2008**, *325*, 851−860.

(5) Du, N.; Park, H. B.; Robertson, G. P.; Dal-Cin, M. M.; Visser, T.; Scoles, L.; Guiver, M. D. Polymer nanosieve membranes for CO_2-capture applications. *Nat. Mater.* **2011**, *10*, 372−375.

(6) Carta, M.; Malpass-Evans, R.; Croad, M.; Rogan, Y.; Jansen, J. C.; Bernardo, P.; Bazzarelli, F.; McKeown, N. B. An efficient polymer molecular sieve for membrane gas separations. *Science* **2013**, *339*, 303−307.

(7) Carta, M.; Croad, M.; Malpass-Evans, R.; Jansen, J. C.; Bernardo, P.; Clarizia, G.; Friess, K.; Lanc, M.; McKeown, N. B. Triptycene induced enhancement of membrane gas selectivity for microporous Troger's base polymers. *Adv. Mater.* **2014**, *26*, 3526−3531.

(8) Ghanem, B.; Swaidan, R.; Ma, X.; Litwiller, E.; Pinnau, I. Energy-efficient hydrogen separation by AB-type ladder-polymer molecular sieves. *Adv. Mater.* **2014**, *26*, 6696−6700.

(9) Swaidan, R.; Ghanem, B.; Litwiller, E.; Pinnau, I. Physical aging, plasticization and their effects on gas permeation in "rigid" polymers of intrinsic microporosity. *Macromolecules* **2015**, *48*, 6553−6561.

(10) Overberger, C. G.; Moore, J. A. Ladder polymers. *Adv. Polym. Sci.* **1970**, *7*, 113−150.

(11) Schlüter, A. D. Ladder Polymers: The new generation. *Adv. Mater.* **1991**, *3*, 282−291.

(12) Scherf, U.; Müllen, K. The synthesis of ladder polymers. *Adv. Polym. Sci.* **1995**, *123*, 1−40.

(13) Scherf, U.; Müllen, K. Polyarylenes and poly(arylenevinylenes), 7. A soluble ladder polymer via bridging of functionalized poly(*p*-phenylene)-precursors. *Makromol. Chem., Rapid Commun.* **1991**, *12*, 489−497.

(14) Tour, J. M.; Lamba, J. J. S. Synthesis of planar poly(p-phenylene) derivatives for maximization of extended pi.-conjugation. *J. Am. Chem. Soc.* **1993**, *115*, 4935−4936.

(15) Schlüter, A. D.; Löffler, M.; Enkelmann, V. Synthesis of a fully unsaturated all-carbon ladder polymer. *Nature* **1994**, *368*, 831−834.

(16) Goldfinger, M. B.; Swager, T. M. Fused Polycyclic Aromatics via Electrophile-Induced Cyclization Reactions: Application to the Synthesis of Graphite Ribbons. *J. Am. Chem. Soc.* **1994**, *116*, 7895−7896.

(17) Scherf, U. Ladder-type materials. *J. Mater. Chem.* **1999**, *9*, 1853−1864.

(18) Lamba, J. J. S.; Tour, J. M. Imine-Bridged Planar Poly(p-phenylene) Derivatives for Maximization of Extended. pi.-Conjugation. The Common Intermediate Approach. *J. Am. Chem. Soc.* **1994**, *116*, 11723−11736.

(19) Chmil, K.; Scherf, U. Conjugated all-carbon ladder polymers: improved solubility and molecular weights. *Acta Polym.* **1997**, *48*, 208−211.

(20) Buey, J.; Swager, T. M. Three-Strand Conducting Ladder Polymers: Two-Step Electropolymerization of Metallorotaxanes. *Angew. Chem., Int. Ed.* **2000**, *39*, 608−612.

(21) Swager, T. M.; Long, T. M.; Williams, V.; Yang, J. S. Polymers containing iptycenes. *Polym. Mater. Sci. Eng.* **2001**, *84*, 304−305.

(22) Plumhof, J. D.; Stöferle, T.; Mai, L.; Scherf, U.; Mahrt, R. F. Room-temperature Bose−Einstein condensation of cavity exciton−polaritons in a polymer. *Nat. Mater.* **2013**, *13*, 247−252.

(23) Tao, L.; Yang, H.; Liu, J.; Fan, L.; Yang, S. Synthesis and Characterization of Fluorinated Bisphenols and Tetraphenols via a Simple One-Pot Reaction. *Synth. Commun.* **2013**, *43*, 2319−2324.

(24) Olvera Garza, L.; Zolotukhin, M.; Hernández-Cruz, O.; Fomine, S.; Cárdenas, J.; Gaviño-Ramírez, R.; Ruiz-Trevino, A. F. Linear, single-strand heteroaromatic polymers from superacid catalyzed step-growth polymerization of ketones with bisphenols. *ACS Macro Lett.* **2015**, *4*, 492−494.

(25) López, G.; Cruz, O.; Olvera Garza, L.; Zolotukhin, M. G.; Fomine, S. Mechanistic aspects of superacid mediated condensation of polyphenols with ketones. Implications for polymer synthesis. *J. Mol. Model.* **2014**, *20*, 2474.

(26) Guzman-Gutierrez, M. T.; Nieto, D. R.; Fomine, S.; Morales, S. L.; Zolotukhin, M. G.; Hernandez, M. C.; Kricheldorf, H. R.; Wilks, E. S. Dramatic enhancement of superacid-catalyzed polyhydroxyalkylation reactions. *Macromolecules* **2011**, *44*, 194−202.

(27) Wolinski, K.; Hinton, J. F.; Pulay, P. Efficient Implementation of the Gauge-Independent Atomic Orbital Method for NMR Chemical Shift Calculations. *J. Am. Chem. Soc.* **1990**, *112*, 8251−8260.

(28) Chai, J.-D.; Head-Gordon, M. Long-range corrected hybrid density functionals with damped atom-atom dispersion corrections. *Phys. Chem. Chem. Phys.* **2008**, *10*, 6615−6620.

(29) Liu, P.; Goddard, J. D.; Arsenault, G.; Gu, J.; McAlees, A.; McCrindle, R.; Robertson, V. Theoretical studies of the conformations and ^{19}F NMR spectra of linear and a branched perfluorooctanesulfonamide (PFOSAmide). *Chemosphere* **2007**, *69*, 1213−1220.

(30) Sanchez-García, S.; Ruiz-Treviño, F. A.; Aguilar-Vega, M. J.; Zolotukhin, M. G. Gas permeability and selectivity in thermally modified poly (oxyindole biphenylyene) membranes bearing a tert-butyl carbonate group. *Ind. Eng. Chem. Res.* **2016**, *55*, 7012−7020.

(31) Robeson, L. M. The upper bound revisited. *J. Membr. Sci.* **2008**, *320*, 390−400.

(32) Cruz, A. R.; Hernandez, M. C.; Guzmán-Gutiérrez, M. T.; Zolotukhin, M. G.; Fomine, S.; Morales, S. L.; Kricheldorf, H. R.; Wilks, E. S.; Cárdenas, J.; Salmón, M. Precision Synthesis of Narrow Polydispersity, Ultrahigh Molecular Weight Linear Aromatic Polymers by $A_2 + B_2$ Nonstoichiometric Step-Selective Polymerization. *Macromolecules* **2012**, *45*, 6774−6780.

DOI: 10.1021/acs.macromol.7b01413
Macromolecules 2017, 50, 8480−8486